

# Resting-state EEG in the Vestibular Region Can Predict Motion Sickness Induced by a Motion-Simulated in-car VR Platform

Gang Li  
*School of Psychology and Neuroscience*  
*University of Glasgow*  
Glasgow, Scotland  
Gang.Li@glasgow.ac.uk

Yu-Kai Wang  
*School of Computer Science*  
*University of Technology, Sydney*  
Sydney, Australia  
YuKai.Wang@uts.edu.au

Mark McGill  
*School of Computing Science*  
*University of Glasgow*  
Glasgow, Scotland  
Mark.McGill@glasgow.ac.uk

Katharina Pöhlmann  
*KITE Research Institute*  
*University of Toronto*  
Toronto, Canada  
katharina.pohlmann@uhn.ca

Stephen Brewster  
*School of Computing Science*  
*University of Glasgow*  
Glasgow, Scotland  
Stephen.Brewster@glasgow.ac.uk

Frank Pollick  
*School of Psychology and Neuroscience*  
*University of Glasgow*  
Glasgow, Scotland  
Frank.Pollick@glasgow.ac.uk

**Abstract**—Monitoring in-car VR motion sickness (VRMS) by neurophysiological signals is a formidable challenge due to unavoidable motion artifacts caused by the moving vehicle and necessary physical movements by the user to interact with the VR environment. Therefore, this paper for the first time investigates if resting-state neurophysiological features and self-reports of stress levels collected prior to exposure to a motion-simulated in-car VRMS induction platform could predict final motion sickness ratings. Our results of linear regression modeling show that the traditional EEG power spectrum was the only resting-state feature set that could predict in-car VRMS ratings. Further, the best regression result was achieved by beta power spectrum in the left parietal area with adjusted  $R^2=22.6\%$  versus  $11.6\%$  in the right. This result not only confirmed the left parietal involvement in motion sickness susceptibility observed in a previous resting-state fMRI study, but also advanced that methodology to mobile neurotechnologies, represented by mobile EEG, referenced by other types of resting-state features. Together, this study may offer a new mobile neurotechnology-based approach to predict passengers' VRMS levels before they start to use VR apps in a moving vehicle.

**Keywords**—EEG, cognitive load, stress level, in-car VR motion sickness, linear regression

## I. INTRODUCTION

Passengers travelled over 873 billion km in the UK in 2019, with imminent advances such as autonomous cars (a market expected to reach \$42 billion by 2025), as well as high-speed public transit like HS2, meaning that this figure will further increase. Consequently, more people will be passengers wanting to fill their travel time usefully, rather than it just being wasted. However, many travellers get sick when they read, work, or play games while in motion, and therefore fail to use their travel time productively. This is especially pertinent when they use VR headset to perform aforementioned in-car activities [1], [2].

Motion sickness caused by the use of VR in a vehicle (termed in-car VR motion sickness, in-car VRMS for short) is a new type of motion sickness that challenges all existing methodologies of monitoring and mitigation that are rooted in either pure motion sickness (that is, pure physical motion-induced motion sickness) or pure cybersickness (that is, pure visually-induced motion sickness). Therefore this study for

the first time investigated if resting-state neurophysiological features and self-reports of stress levels collected prior to exposure to a motion-simulated in-car VRMS induction platform could predict final motion sickness ratings. These neurophysiological features are 1) resting-state EEG features (including traditional power spectrum and inter-trial coherence) extracted from vestibular regions and 2) cognitive load estimated from pupillometry and forehead photoplethysmography (PPG).

If this study is successful and suggesting that it is feasible to predict passengers' in-car VRMS susceptibility through their resting-state neurophysiological signals collected prior to the in-car VR experience, then a personalized in-car VRMS mitigation countermeasure can be developed to make the consumption of VR in a moving vehicle a comfortable (motion sickness free) and productive experience. For example, if an individual's susceptibility to motion sickness is low, then standalone behavioural treatments (like music, airflow and smell) [3]–[5] are perhaps adequate without the need to redesign the existing VR contents; otherwise perhaps a context-aware VR app that can more strongly mitigate in-car VRMS, such as through synchronizing the car movements and VR content presentation [6] would be necessary. This is especially pertinent given estimates that the market of in-car VR applications will reach 14\$ billion globally by 2027.

## II. RELATED WORK AND OUR CONTRIBUTIONS

Visual-vestibular sensory conflict theory is a widely-accepted proposal to explain the aetiology of motion sickness [7]. Mounting evidence has shown that neural biomarkers extracted from vestibular areas are significantly associated with the perceived severity of motion sickness, no matter if it is pure cybersickness (such as VRMS) [8]–[10] or pure motion sickness [11]. However, these biomarkers are all extracted while exposed to a motion sickness inducing stimuli, very few studies focused on the feasibility of using resting-state neural biomarkers to predict motion sickness. A more recent study is the first study on this topic [12]. Authors adopted resting-state MRI to understand the different brain activity patterns between participants who are susceptible and resistant to pure motion sickness. They found that the left parietal area is significantly correlated with participants' susceptibilities evaluated by the motion sickness susceptibility questionnaires (MSSQ) based on their past experience [13].

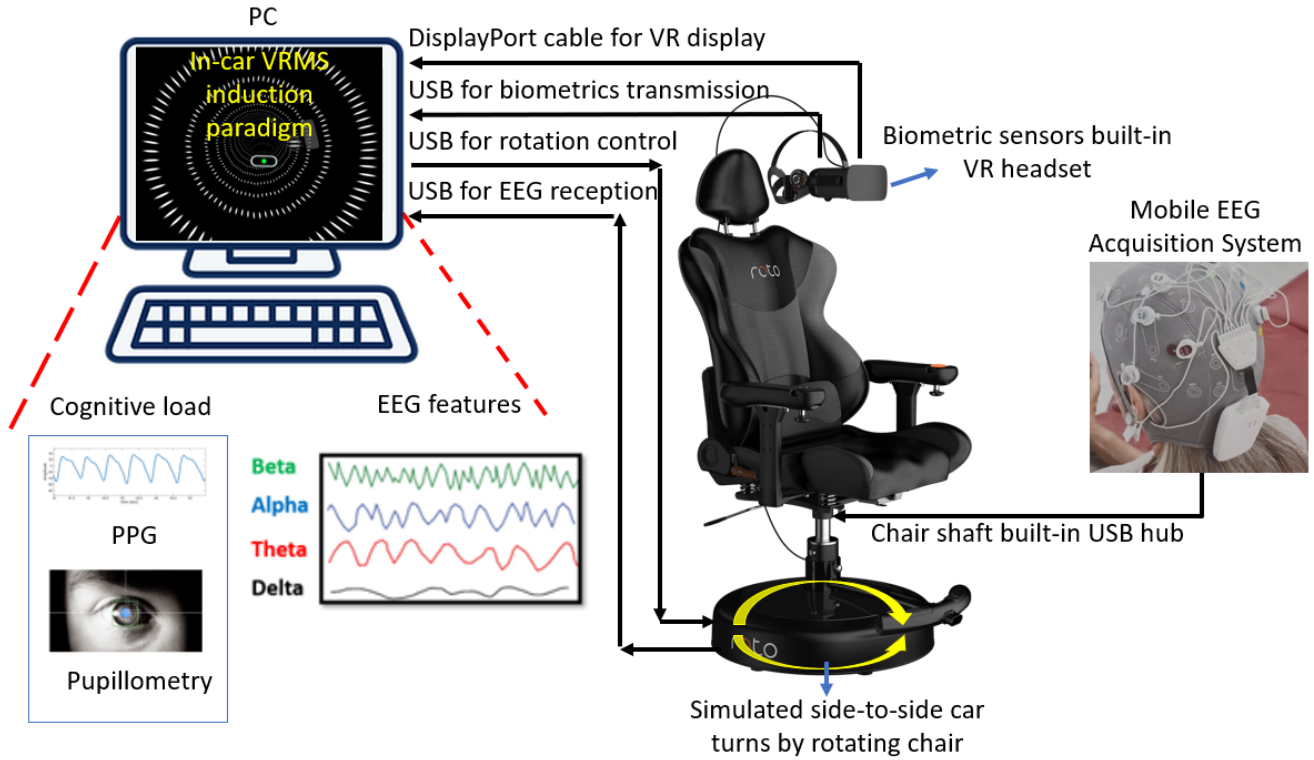


Fig. 1 The system architecture of our in-car VRMS induction platform, where the cognitive load was estimated by a VR built-in commercial machine learning model through combined PPG and pupillometry signals (see [16]).

Built on this early evidence, our goal was to take one step further to investigate if resting-state mobile neurotechnology-based biomarkers (that is, low-density resting-state EEG features in the vestibular region) could predict participants' motion sickness ratings obtained through a motion-simulated in-car VR platform rather than self-reported motion sickness history (such as MSSQ). Also, evidence has shown that peripheral physiological signals and emotions are associated with motion sickness [8], [14], [15]. Therefore, our study compared two additional types of resting-state features (that is, cognitive load estimated from peripheral physiological signals and self-reported stress levels) with EEG features, in order to justify EEG features more fairly.

### III. SIMULATED IN-CAR VRMS INDUCTION PLATFORM

#### A. System Architecture

As can be seen in Fig. 1, our simulated in-car VRMS induction platform consists of a PC, a rotating chair (RotoVR), a PC-powered biometric sensors built-in VR headset (HP VR headset Reverb G2 Omnicept Edition) as well as a mobile EEG device (StarStim8, Neuroelectronics, Spain).

The PC is equipped with a NVIDIA GeForce RTX 2070 GPU that can run HP Reverb G2 Omnicept Edition at full resolution (that is, 4320 x 2160 pixels combined / 2160 x 2160 per eye). This headset was chosen for this study as it can estimate real-time cognitive load by its built-in biometrics sensors (Tobii eye-tracking sensors and forehead near-infrared green light PPG sensor) and a PC-based machine learning model. This machine learning model was built based on 738 participants with an average classification accuracy of 79.08% without calibration. HP researchers claimed that this model is novel and can reliably estimate cognitive load in the general population in comparison to past research. More details can be found in HP's technical report [16]. StarStim8

is an 8-channel mobile EEG acquisition system with a high-resolution, high-speed analog-to-digital converter (24-bit at 500Hz sampling rate). StarStim supports WiFi, but communication failure occurs occasionally, therefore we used a USB cable instead throughout the whole study. However, this brought on a problem, that is, the EEG USB cable can be entangled between the PC and the rotating chair when the rotating chair was rotating. Thus, we selected RotoVR rotating chair (RotoVR 1.0, London, UK) which is equipped with a USB hub at its chair shaft by which the EEG USB cable is separated from the PC and relatively stationary with the chair but the EEG signals can still be transmitted (relayed) to PC end by another USB cable connected with the fixed chair base. More importantly, RotoVR comes with a VR SDK which can be used by VR app developers to control RotoVR's rotation directly through a widely-used VR development engine — Unity 3D.

#### B. In-car VRMS Induction Paradigm

According to Griffin's model of motion sickness [17], motion sickness can be classified into three categories. Type I: motion sickness caused by motion that is felt but not seen, such as traditional car sickness — reading a book in a moving car. Type II: motion sickness caused by motion that is seen but not felt, such as pure cybersickness [18]. Type III: motion sickness caused when both visual and vestibular systems detect motion but they are uncorrelated with each other, such as Coriolis rotation, that is, during constant speed rotation of the body and head rotation about an axis other than the axis of rotation of the body [19], motion sickness experienced when using in-car VR therefore is just a 21st century version of Coriolis rotation. What is distinctive about in-car VRMS is that the discrepancy between visual and vestibular systems can be caused by uncorrelated visual motion presented in VR and physical body motion induced by car turns simulated by

yaw rotations of the RotoVR rotating chair in this study), without necessarily requiring the body and head to rotate on different axes.

Our in-car VRMS induction was based on the mixture of a visual tunnel travel tasks presented in VR that elicited self-forward motion and physical yaw rotations by the rotating chair. This mixture causes the visual system to receive sensory input for linear motion while the vestibular system receives sensory input for angular motion, resulting in conflict between visual and vestibular sensory inputs. This paradigm can be viewable by this Youtube link: [https://youtu.be/aw\\_ZT\\_c6qeo](https://youtu.be/aw_ZT_c6qeo).

The rotation frequency of the chair was random but less than 0.2Hz, which is a commonly-used frequency range to induce motion sickness [20]. The tunnel travel task was adapted from a well-established multitasking cognitive task, NeuroRacer [21], where the participant's multitasking performance was assessed by challenging visual discrimination ability in the context of visuomotor tracking. For the visual discrimination (sign task), participants were instructed to selectively respond to the target sign (green circle) as fast as possible by pressing the trigger button on the left VR controller and ignoring other non-target signs including green pentagons and squares; blue and red circles, pentagons, and squares. For the visuomotor tracking (hitting task), participants were required to hit the centre of the grey box as accurately as possible by moving the thumbstick on the right VR controller. The position of the grey box was randomly placed on the circumference of the tunnel cross-section (see the screenshot over the PC icon in Fig. 1).

We adopted a multitasking cognitive task-integrated tunnel travel task rather than a pure tunnel travel task because this cognitive task contains an adaptive staircase algorithm (see our previous paper [22]) to adjust the difficulty of the task so that participant's cognitive load can be maintained approximately the same. Simply, we do not hope that the cognitive load during in-car VRMS induction would be a variable as cognitive load is a co-founding factor that can affect participant's susceptibility [23].

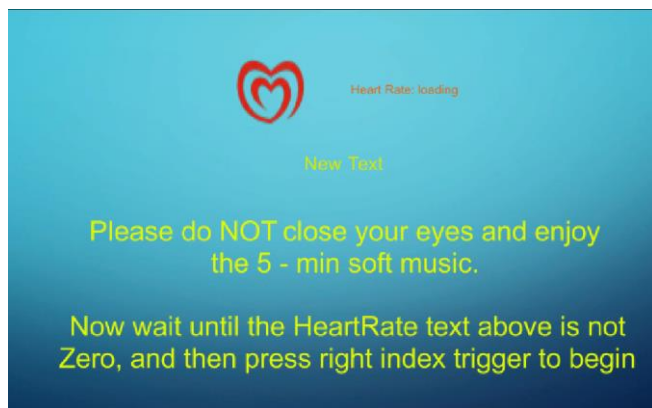


Fig. 2 The resting-state EEG paradigm where participants were instructed to listen to a piece of soft music by pressing a button on the VR controller after their heart rate is loaded and displayed to them. This simple biofeedback mechanism can better help them get into the resting-state mood. In this screenshot, "New Text" is where the 5-minute countdown timer would be if this was an ongoing experiment.

### C. The Resting-State Paradigm

The "resting state" here specifically refers to asking participants to listen to a piece of soft music (copyrighted

from a local beauty salon in China) with their eyes open viewing a blue bulletin board (see Fig.2), during which the rotating chair remained stationary. This bulletin board can display a participant's heart rate to them through a textbox (such as "Heart Rate: 77") next to the heart shape at the top, thus can better help participants get into the resting-state mood. This approach differs from past resting-state research in which participants were solely verbally instructed to do not think of anything [12].

## IV. METHOD

### A. Participants

Thirty-nine gender-balanced non-VR/PC game players aged between 20-30 were recruited (19 females and 20 males), where non-VR/PC game players were defined as spending less than 2 hours a month engaging in VR and PC games.

### B. Experimental Procedure

Before the 30-min in-car VRMS induction, the 5-min resting-state of EEG signals were recorded, and at the same time pupillometry and forehead PPG signals were collected. During the in-car VRMS induction, participants' self-reports of VRMS ratings (that is, fast motion sickness scale [24], FMS for short) were collected every 3 minutes, where FMS is a scale of 0 (unnoticeable nausea and general discomfort) to 20 (intolerable nausea and general discomfort). According to our ethics committee's suggestion, a threshold of FMS=10 was set to induce moderate in-car VRMS, otherwise we had to stop the ongoing experiment immediately. FMS ratings obtained right before the end of VRMS induction (or right before they dropped out) were used for statistical analysis. The full study protocol was approved by the ethics committee of the University of Glasgow (No. 300200243). Participants read the privacy notice and participant information sheet onsite and gave informed consent prior to participation. Participants received £10 per hour for participation.

### C. EEG Settings, Pre-processing and Feature Extraction

Four conductive gel-based wet electrodes were used and placed at the vestibular region of interest. To be more specific, that is, P3 and P4-based parieto-insular vestibular cortex (PIVC) and CP5 and CP6-based temporoparietal junction (TPJ) [11], [25]–[27], as shown in Fig. 3. The ground and reference electrodes were connected and placed on the right earlobe by an ear clip.

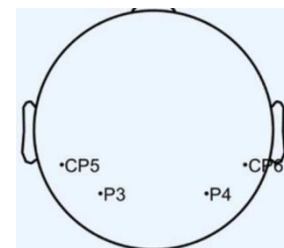


Fig. 3 The system-generated EEG channel location by EEGLab

For EEG pre-processing, a low-pass filter with a cutoff frequency of 30 Hz and high-pass filter with a cutoff frequency of 0.1 Hz were applied to remove power line noise

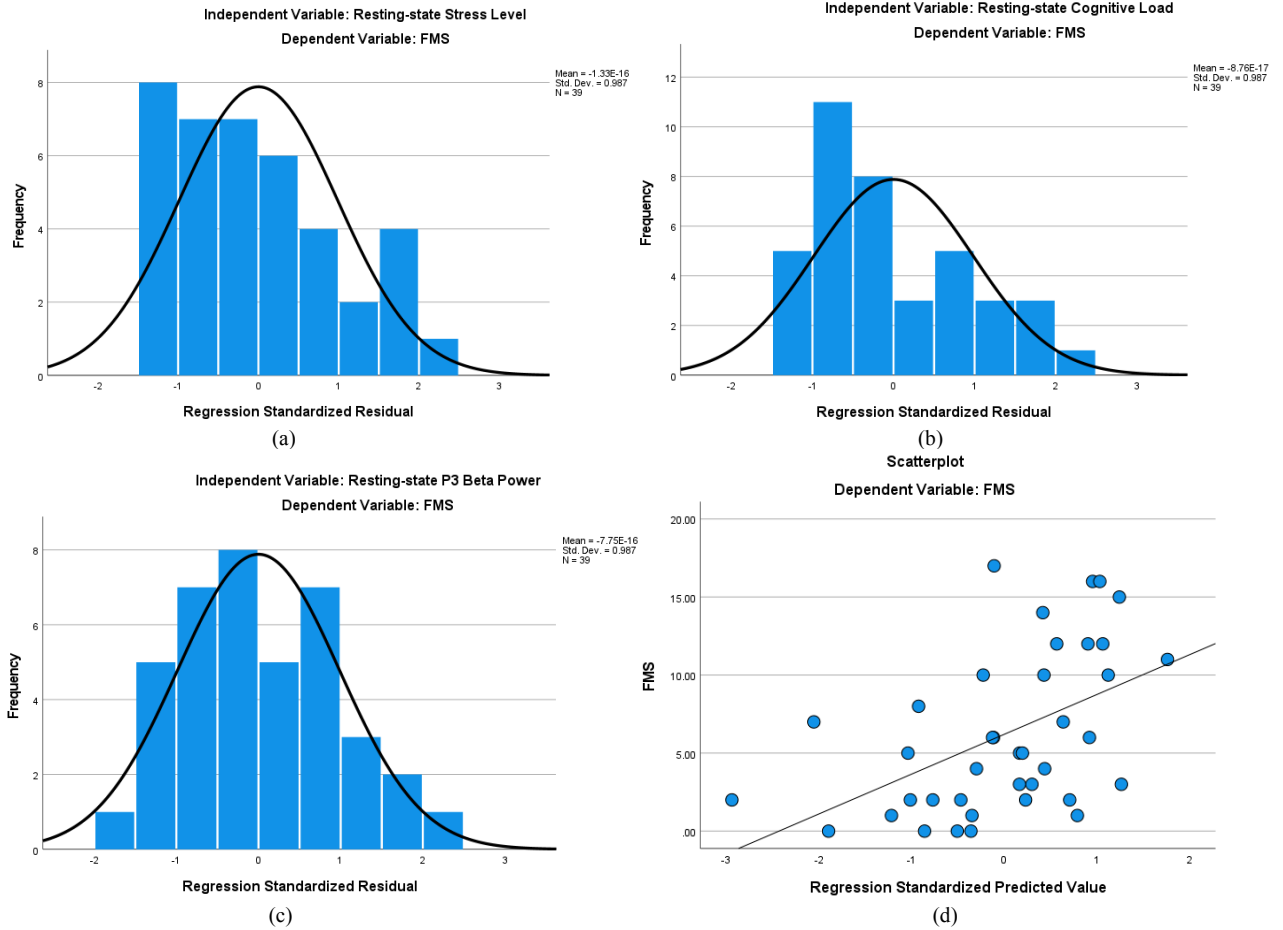


Fig. 4 The results of predicting FMS ratings using linear regression model and resting-state neurophysiological features (a) - (c) the histograms of regression residuals using resting-state cognitive load, stress level and EEG P3-Beta power, respectively. (d) the scatter plot of original FMS and predicted FMS ratings using resting-state EEG P3-Beta power.

and DC drift, respectively. The filtered EEG data were then corrected using the mean of each channel and then 200-s long EEG data right before the end of resting-state EEG was extracted as the targeted resting-state EEG for further feature extraction. Ultimately, all 200-s long targeted resting-state EEG epochs were segmented into 100 2-s epochs and all epochs were cleaned of excessive peak-to-peak deflections, amplifier clippings, and other artifacts, using a voltage threshold of 100  $\mu$ V.

TABLE I. SUMMARY OF EEG FEATURES USED IN THIS STUDY

Region of interest	Feature	Implication
Left and Right PIVC (P3 and P4) ; Left and Right TPJ (CP5 and CP6)	Power spectrum	Averaged amplitude changes of EEG segments in a certain frequency band
	Inter-trial coherence (ITC)	Averaged phase changes between EEG segments in a certain frequency band

EEG features shown in Table I were extracted respectively, where the definitions for EEG frequency bands were: Delta (0.1–3 Hz), Theta (4–7 Hz), Alpha (8–12 Hz) and Beta (13–30 Hz). As the traditional power spectrum and ITC features measure amplitude and phase information of the EEG dynamics, respectively, we can compare the resting-state features of EEG in terms of amplitude and phase to examine which one can better predict in-car VRMS.

All EEG pre-processing and feature extraction procedures were carried out in a batch processing manner through custom MATLAB scripts and/or EEGLab v2022. (an open-source MATLAB plugin developed by Swartz Center for Computational Neuroscience; [www.sccn.ucsd.edu/eeGLab](http://www.sccn.ucsd.edu/eeGLab)).

#### D. Predictive Model

A linear regression modeling procedure with stepwise algorithm-based predictor selection function in SPSS 28.0.0.0 was used. Since the sample size is  $N=39$  (this is, the number of participants), and the number of potential predictor is  $N=16$  (that is, the number of EEG features,  $N=\text{the number of EEG channels} \times \text{the number of EEG frequency bands}=4 \times 4=16$ ), therefore, in order to avoid violating the principle of approximately ten samples per predictor in the regression [28], [29], we adopted stepwise regression to select maximum 3 best predictors to build our final linear regression model. The statistical significance threshold was set as  $p < 0.05$ .

### V. RESULTS

#### A. Resting-state Cognitive Load and Stress Levels

Neither resting-state cognitive load nor stress levels could establish a significant regression relationship with FMS ratings with adjusted  $R^2=-0.024$ ,  $F_{1,38}=0.116$  and  $p=0.735$  for cognitive load and adjusted  $R^2=0.039$ ,  $F_{1,38}=2.562$  and  $p=0.118$  for stress levels. As shown in Fig. 4 (a) and (b), their histograms of regression residuals do not belong to normal distribution.

## B. Resting-state EEG features

1) *Power spectrum*: We found that beta power at P3 could establish the best regression model to predict FMS ratings with adjusted  $R^2=0.226$ ,  $F_{1,38}=12.105$  and  $p=0.001$ . The specific coefficients are as follows:

$$FMS=15.057+336.666*P3_{Beta\_Power} \quad (1)$$

Where, 15.057 is the constant with  $p<0.001$ , 336.666 is the regression coefficient with  $p=0.001$ . The histogram of regression residuals and predicted FMS ratings can be found in Fig. 4 (c) and (d).

Note: In our stepwise regression analyses,  $P3_{Beta\_power}$  is the EEG feature showing the best regression relationship, but not the only one that can establish a significant regression model, such as  $P4_{Beta\_power}$  with adjusted  $R^2=0.116$ ,  $F_{1,38}=5.986$  and  $p=0.019$ . The specific coefficients are as follows:

$$FMS=12.149+235.686*P4_{Beta\_Power} \quad (2)$$

Taken Sakai et al [12]'s findings together, these results confirmed that resting-state brain activity patterns in the left parietal area indeed can predict motion sickness susceptibility.

2) *ITC*: We did not find any ITC features that could achieve a significant regression relationship to predict FMS ratings.

## VI. DISCUSSION

### A. Resting-state EEG vs Resting-state non-EEG features

In our previous study [14], we found that peripheral physiological features (such as heart rate and fingertip temperature) outperformed EEG features in predicting motion sickness when recorded throughout exposure to sickness inducing stimuli; however the present work found the opposite in the context of resting-state analyses, indicating the uniqueness of resting-state EEG signals on predicting motion sickness if compared to resting-state peripheral signals. Taken together, these results suggest that EEG signals are more suitable for predicting motion sickness prior to its onset thereby supporting the prevention of motion sickness, while peripheral signals are more suitable for real-time monitoring of motion sickness symptoms during exposure. However, neither type of signal established a strong regression model, according to their adjusted  $R^2$  values ( $<0.3$  while strong one should be  $>0.7$ ).

### B. Resting-state EEG vs stimuli-related EEG features

In a previous study [8], we found that stimuli-related EEG features could achieve a strong regression model with an adjusted  $R^2=0.875$ ; while the present work established a weak one with an adjusted  $R^2=0.226$ . Our reasoning behind this phenomenon is that this is a normal situation that can reflect the causality of EEG features in describing the severity of motion sickness, after all stimuli-related EEG features are much closer to the timing of self-reported sickness ratings.

Note, we did not cite other studies in this section because we managed to compare our results in the context of similar

motion sickness stimuli (tunnel travel), the same EEG device (StarStim8) and a similar group of participants (20-30 yrs non-VR/PC game players).

## C. Limitation

Although we found that resting-state  $P3_{Beta\_Power}$  could predict VRMS induced by our motion-simulated in-car VR platform, it is still unknown whether this finding can be transferred to other in-car VR platforms (and other VRMS induction paradigms). Particularly, since wearing discomfort per se also can trigger VRMS (such as, the tightness of the VR headset), other VR headsets may not show the same EEG pattern. However, we still believe that our finding is representative because the brain region and EEG frequency band are all consistent with previous studies where authors used different neuroimaging technique (such as fMRI [12]) and VR headsets (such as Quest 2 [8]) than ours. However, this finding, from an applied perspective, is not user-friendly because of the use of conductive gel and an EEG cap. Therefore, future study should incorporate a comparative analysis involving state-of-the-art VR display technologies to highlight the uniqueness of our EEG-based finding. For example, as in [30], if the VR display is free of vergence-accommodation conflict, will the VRMS be milder? Another example, as in [31], if the contents or graphics can be processed in a way analogous to the human brain, will the VRMS be cured?

## VII. CONCLUSION

The emerging in-car VR use cases highlight the need for a way to predict passengers' VRMS levels in advance of their journeys to avoid severe symptoms of VRMS later on. To do so, this paper investigated the feasibility of using resting-state EEG features to predict the final in-car VRMS ratings obtained through a simulated in-car VR platform. We found that indeed resting-state EEG features are able to predict those sickness ratings, and the best prediction result was achieved by beta power in the left parietal area.

## ACKNOWLEDGMENT

This work was supported in part by the European Research Council (ERC) through the European Union's Horizon 2020 Research and Innovation Programme under Grant 835197, and in part by the Royal Society of Edinburgh under SAPHIRE Grant 2832. A special thanks to Prof. Ian M. Thornton of Department of Cognitive Science, University of Malta, and Alana Grant of School of Computing Science, University of Glasgow, for their help in the design of in-car VR platform and in-car VRMS induction paradigm for this study.

## REFERENCES

- [1] M. McGill, A. Ng, and S. Brewster, "I Am The Passenger: How Visual Motion Cues Can Influence Sickness For In-Car VR," in *Proceedings of the 2017 CHI Conference on Human Factors in Computing Systems*, Denver Colorado USA: ACM, May 2017, pp. 5655–5668. doi: 10.1145/3025453.3026046.
- [2] J. Li, C. George, A. Ngao, K. Holländer, S. Mayer, and A. Butz, "An Exploration of Users' Thoughts on Rear-Seat Productivity in Virtual Reality," in *12th International Conference on Automotive User Interfaces and Interactive Vehicular Applications*, in *AutomotiveUI '20*. New York, NY, USA: Association for Computing Machinery, Sep. 2020, pp. 92–95. doi: 10.1145/3409251.3411732.
- [3] S. D'Amour, J. E. Bos, and B. Keshavarz, "The efficacy of airflow and seat vibration on reducing visually induced motion sickness," *Exp*



- Brain Res.*, vol. 235, no. 9, pp. 2811–2820, Sep. 2017, doi: 10.1007/s00221-017-5009-1.
- [4] “Examining potential effects of arousal, valence, and likability of music on visually induced motion sickness | SpringerLink.” Accessed: Jul. 29, 2023. [Online]. Available: <https://link.springer.com/article/10.1007/s00221-020-05871-2>
  - [5] B. Keshavarz, D. Stelzmann, A. Paillard, and H. Hecht, “Visually induced motion sickness can be alleviated by pleasant odors,” *Exp Brain Res*, vol. 233, no. 5, pp. 1353–1364, May 2015, doi: 10.1007/s00221-015-4209-9.
  - [6] M. McGill, G. Wilson, D. Medeiros, and S. A. Brewster, “PassengXR: A Low Cost Platform for Any-Car, Multi-User, Motion-Based Passenger XR Experiences,” in *Proceedings of the 35th Annual ACM Symposium on User Interface Software and Technology*, in UIST ’22. New York, NY, USA: Association for Computing Machinery, Oct. 2022, pp. 1–15. doi: 10.1145/3526113.3545657.
  - [7] J. T. Reason, “Motion sickness adaptation: a neural mismatch model,” *J R Soc Med*, vol. 71, no. 11, pp. 819–829, Nov. 1978.
  - [8] G. Li *et al.*, “Multimodal Biosensing for Vestibular Network-Based Cybersickness Detection,” *IEEE Journal of Biomedical and Health Informatics*, pp. 1–1, 2021, doi: 10.1109/JBHI.2021.3134024.
  - [9] S. Nam, K.-M. Jang, M. Kwon, H. K. Lim, and J. Jeong, “Electroencephalogram microstates and functional connectivity of cybersickness,” *Frontiers in Human Neuroscience*, vol. 16, 2022, Accessed: Oct. 18, 2022. [Online]. Available: <https://www.frontiersin.org/articles/10.3389/fnhum.2022.857768>
  - [10] M. Nürnberger, C. Klingner, O. W. Witte, and S. Brodoehl, “Mismatch of Visual-Vestibular Information in Virtual Reality: Is Motion Sickness Part of the Brains Attempt to Reduce the Prediction Error?,” *Frontiers in Human Neuroscience*, vol. 15, 2021, Accessed: Mar. 07, 2023. [Online]. Available: <https://www.frontiersin.org/articles/10.3389/fnhum.2021.757735>
  - [11] Q. Arshad *et al.*, “Electrocortical therapy for motion sickness,” *Neurology*, vol. 85, no. 14, pp. 1257–1259, Oct. 2015, doi: 10.1212/WNL.0000000000001989.
  - [12] H. Sakai *et al.*, “Left parietal involvement in motion sickness susceptibility revealed by multimodal magnetic resonance imaging,” *Hum Brain Mapp*, vol. 43, no. 3, pp. 1103–1111, Nov. 2021, doi: 10.1002/hbm.25710.
  - [13] J. F. Golding, “Motion sickness susceptibility questionnaire revised and its relationship to other forms of sickness,” *Brain Res Bull*, vol. 47, no. 5, pp. 507–516, Nov. 1998, doi: 10.1016/s0361-9230(98)00091-4.
  - [14] G. Li, O. Onuoha, M. McGill, S. Brewster, C. P. Chen, and F. Pollick, “Comparing Autonomic Physiological and Electroencephalography Features for VR Sickness Detection Using Predictive Models,” in *2021 IEEE Symposium Series on Computational Intelligence (SSCI)*, IEEE, 2021, pp. 01–08.
  - [15] M. Kaufeld, J. Bourdeinik, L. M. Prinz, M. Mundt, and H. Hecht, “Emotions are associated with the genesis of visually induced motion sickness in virtual reality,” *Exp Brain Res*, vol. 240, no. 10, pp. 2757–2771, Oct. 2022, doi: 10.1007/s00221-022-06454-z.
  - [16] Siegel, E.H. *et al.*, “HP Omnicept Cognitive Load Database (HPO-CLD) – Developing a Multimodal Inference Engine for Detecting Real-time Mental Workload in VR.” HP Labs, 2021. Accessed: Feb. 10, 2023. [Online]. Available: <https://developers.hp.com/omnicept/hp-labs-omnicept-cognitive-load-inference-dataset>
  - [17] M. Griffin, “Handbook of Human Vibration.” Accessed: Feb. 07, 2023. [Online]. Available: <https://shop.elsevier.com/books/handbook-of-human-vibration/griffin/978-0-12-303041-2>
  - [18] M. E. McCauley and T. J. Sharkey, “Cybersickness: Perception of self-motion in virtual environments,” *Presence: Teleoper. Virtual Environ.*, vol. 1, no. 3, pp. 311–318, Jan. 1992.
  - [19] W. Bles, “Coriolis effects and motion sickness modelling,” *Brain Research Bulletin*, vol. 47, no. 5, pp. 543–549, Nov. 1998, doi: 10.1016/S0361-9230(98)00089-6.
  - [20] J. F. Golding, A. G. Mueller, and M. A. Gresty, “A motion sickness maximum around the 0.2 Hz frequency range of horizontal translational oscillation,” *Aviation, Space, and Environmental Medicine*, vol. 72, no. 3, Art. no. 3, Mar. 2001, Accessed: Apr. 24, 2023. [Online]. Available: <https://westminsterresearch.westminster.ac.uk/item/93zwx/a-motion-sickness-maximum-around-the-0-2-hz-frequency-range-of-horizontal-translational-oscillation>
  - [21] J. A. Anguera *et al.*, “Video game training enhances cognitive control in older adults,” *Nature*, vol. 501, no. 7465, Art. no. 7465, Sep. 2013, doi: 10.1038/nature12486.
  - [22] G. Li, J. A. Anguera, S. V. Javed, M. A. Khan, G. Wang, and A. Gazzaley, “Enhanced Attention Using Head-mounted Virtual Reality,” *J Cogn Neurosci*, vol. 32, no. 8, pp. 1438–1454, Aug. 2020, doi: 10.1162/jocn\_a\_01560.
  - [23] K. Pohlmann, J. F. H. A. Maior, L. O’Hare, A. Parke, A. Landowska, and P. Dickinson, “I think I don’t feel sick: Exploring the Relationship Between Cognitive Demand and Cybersickness in Virtual Reality using fNIRS.” Hamburg, Germany, Apr. 23, 2023.
  - [24] B. Keshavarz and H. Hecht, “Validating an efficient method to quantify motion sickness,” *Hum Factors*, vol. 53, no. 4, pp. 415–426, Aug. 2011, doi: 10.1177/0018720811403736.
  - [25] J. Dowsett, C. S. Herrmann, M. Dieterich, and P. C. J. Taylor, “Shift in lateralization during illusory self-motion: EEG responses to visual flicker at 10 Hz and frequency-specific modulation by tACS,” *Eur J Neurosci*, vol. 51, no. 7, pp. 1657–1675, Apr. 2020, doi: 10.1111/ejn.14543.
  - [26] N. Takeuchi, T. Mori, Y. Suzukamo, and S.-I. Izumi, “Modulation of Excitability in the Temporoparietal Junction Relieves Virtual Reality Sickness,” *Cyberpsychol Behav Soc Neww*, vol. 21, no. 6, pp. 381–387, Jun. 2018, doi: 10.1089/cyber.2017.0499.
  - [27] A. Kyriakareli, S. Cousins, V. E. Pettorossi, and A. M. Bronstein, “Effect of transcranial direct current stimulation on vestibular-ocular and vestibulo-perceptual thresholds,” *Neuroreport*, vol. 24, no. 14, pp. 808–812, Oct. 2013, doi: 10.1097/WNR.0b013e3283646e65.
  - [28] B. M. Biccard *et al.*, “Patient care and clinical outcomes for patients with COVID-19 infection admitted to African high-care or intensive care units (ACCCOS): a multicentre, prospective, observational cohort study,” *The Lancet*, vol. 397, no. 10288, pp. 1885–1894, May 2021, doi: 10.1016/S0140-6736(21)00441-4.
  - [29] P. Peduzzi, J. Concato, E. Kemper, T. R. Holford, and A. R. Feinstein, “A simulation study of the number of events per variable in logistic regression analysis,” *J Clin Epidemiol*, vol. 49, no. 12, pp. 1373–1379, Dec. 1996, doi: 10.1016/s0895-4356(96)00236-3.
  - [30] L. Mi, C. P. Chen, Y. Lu, W. Zhang, J. Chen, and N. Maitlo, “Design of lensless retinal scanning display with diffractive optical element,” *Opt Express*, vol. 27, no. 15, pp. 20493–20507, Jul. 2019, doi: 10.1364/OE.27.020493.
  - [31] N. Xi, J. Ye, C. P. Chen, Q. Chu, H. Hu, and S. P. Zou, “Implantable metaverse with retinal prostheses and bionic vision processing,” *Opt Express*, vol. 31, no. 2, pp. 1079–1091, Jan. 2023, doi: 10.1364/OE.478516.